

## Sintering behavior of nano yttria powder compacts fabricated by various forming processes

Yeoung-Gyun Yang<sup>a</sup>, Ji-Yeon Kwak<sup>b</sup>, Heon Kong<sup>c</sup> and Sang-Jin Lee<sup>a,c,\*</sup>

<sup>a</sup>Dept. of Advanced Materials Science and Engineering, Mokpo National University, Muan, Republic of Korea

<sup>b</sup>Dept. of Physiology and Biophysics, Inha University College of Medicine, Incheon, Republic of Korea

<sup>c</sup>Research Institute of Ceramic Industry and Technology, Mokpo National University, Muan, Republic of Korea

The sintering behavior of 10 nm sized, nano yttria powder was investigated with powder compacts prepared by various forming methods with an aqueous system. A well dispersed nano yttria slurry and gelation conditions were determined by examining rheological behavior according to the pH and the amount of dispersant content. Slip casting was performed on the slurry prepared under optimum dispersion conditions. For comparison, the powder compacts were prepared by uni-axially pressing the nano powder and the gel powder. When a granular-type gel powder was applied, dry pressing was conducted with less agglomeration, and the green density was improved, unlike the case of using the nano-powder. The most homogeneous microstructure was observed for the slip casting sample. As a result of sintering at 1650 °C for 2 hours in atmospheric conditions, the green sample prepared by slip casting showed the highest densification of 98% relative density with 41% shrinkage. In particular, fracture behavior and circular pores were present in the intra-granular area, unlike the cases of press formed samples. The powder compact using gel powder showed higher sintered density of 93% compared with the press formed powder compact using nano powder.

**Key words:** Nano yttria, Slip casting, Sintering, Gelation, Powder forming.

### Introduction

As yttria (Y<sub>2</sub>O<sub>3</sub>) has excellent resistance to corrosion and thermal shock and high infrared transmission, it is used for infrared sensors, laser devices, missile protection domes and high temperature solid oxide fuel cells [1–10]. In recent years, research on the production of translucent ceramics using the pressure sintering of yttria has been actively conducted [11, 12]. For this purpose, producing a dense sintered yttria would be the essential process. Although yttria is an oxide ceramic, a high sintering temperature of about 1800 °C is required under normal pressure for densification because yttria has high melting temperature and heat resistance. Therefore, pressure sintering such as HIP (Hot Isostatic Pressing) is used [13]. In order to lower the sintering temperature of yttria, fine nano-sized powder is required. Nano-particles improve the densification during the initial sintering step by the higher surface energy of the powder compact, and this results in denser bulk density at relatively lower temperature [14]. According to a recent report, a high purity yttria powder of about 10 nm has been prepared by a polymer solution method [1–2, 15].

D. Huo et al., prepared a dispersed slurry using yttria powder having an average particle size of 300 nm or less, and the slip casted body was pre-sintered at 1200 °C and then vacuum-sintered at 1700 °C [4]. Depending on the amount of dispersant used in the slurry preparation, there are differences in sintered density. The highest density was obtained with 99.36% when 1.0 wt% dispersant was added. As the amount of the dispersant was increased, the pores in the sintered body were increased, and most of them existed in the intra-grains. According to Y. Xu et al., 5 mol% of ZrO<sub>2</sub> powder was added to the yttria powder having an average of 3 μm, and then a slurry was prepared using ethanol which is a nonpolar solvent. The molded body was then sintered at about 2000 °C for 10 to 15 hours in a vacuum furnace to produce a dense yttria sintered body having a light transmitting property [5].

In the press forming process of nano-powder, the severe agglomeration between particles is caused by the Van Der Waals attraction and the static electricity with the mold. Therefore, it is not easy to obtain the desired green density using the general dry uniaxial pressing method. Agglomerated particles may interfere with the diffusion of pores during the sintering process by sharp edges or uneven surfaces. Further, due to the large pores in the green body caused by the irregular agglomeration, it may be difficult to remove the pores during the firing process [4]. In order to solve this problem, an alternative may be considered by preparing

\*Corresponding author:  
Tel : +82-61-450-2493  
Fax: +82-61-450-2498  
E-mail: lee@mokpo.ac.kr

a suspension in which ceramic nano-particles are dispersed, and forming a green body by the slip casting method using the obtained slurry.

In this paper, the sintering behavior of nano yttria powder of 10 nm size prepared using a polymer solution was investigated. In particular, in order to obtain a densified yttria by pressureless sintering under atmospheric conditions, the yttria green samples were manufactured using various forming methods. As the dry pressing of nano powder is not easy to obtain dense sintered yttria because of poor green body density, alternative methods of slip casting in an aqueous system and granular powder pressing through gelation are introduced. The sintering behavior at a relatively low temperature of around 1600 °C was also examined with the green bodies obtained from the various forming methods.

## Experimental Procedure

### Rheology control of nano yttria powder

To obtain nano yttria powder, yttrium nitrate ( $\text{Y}(\text{NO}_3)_3 \cdot 6\text{H}_2\text{O}$ , reagent grade, Sigma-Aldrich) was dissolved in deionized water, and then 5 wt% PVA solution (MW. 146,000~186,000, polyvinyl alcohol, Sigma-Aldrich Chemical, HEMIE GmbH, USA) was added for homogeneous dispersion of yttrium ions. After drying with stirring, the precursor was calcined at 600 °C for 1 hour. The yttria powder synthesized from the PVA solution method showed a crystallite size of about 10~15 nm with a high surface area of 34.71 m<sup>2</sup>/g [1].

Dispersion behavior of the nano yttria powder in an aqueous system was investigated with variation of the dispersant amount and pH of the slurry. For the experiment, nano yttria powder was mixed with deionized water at a weight ratio of 9:1. The dispersant (polycarboxylic acid type) amount was varied from 0.2 to 1.2 wt% in the slurry. Ball milling was then performed using a 5mm diameter zirconia ball for 24 hours. The mixed solutions were respectively put in 20 ml measuring cylinder, and the sedimentation behavior was examined by measuring the settling height at regular intervals. To examine the dispersion behavior according to the pH, the slurry containing 1.2 wt% of dispersant was adjusted to pH 7.5~10.0. An ammonia solution (pH : 13.7, Junsei Chemical Co., Ltd.) and a 30%-acetic acid solution (pH : 1.6, Daejung Chemicals & Metals Co., LTD) were used as the pH regulators. The 30%-acetic acid solution was added to lower the pH of the solution, while the initial value was lowered, after some time, the pH increased. This was presumably due to the evaporation of the acetic acid, and in response ammonia solution was added to make a buffer. The pH thus could be lowered by adding 30%-acetic acid solution and a small amount of ammonia solution. In this case, the pH of the slurry was not changed even after over 1 hour.

The yttria slurry subjected to gelation by control of

pH was dried at room temperature for 36 hours, and then dried in a dryer at 120 °C, for at least 24 hours to prepare a dried gel. By passing the dried gel through a 200 mesh sieve, a granule-type yttria gel powder having a constant particle size was obtained.

### Forming and sintering

Three kinds of nano yttria powder compacts were prepared and their sintering behavior was investigated. The prepared nano yttria powder and granule-type yttria gel powder were uni-axially pressed, respectively, at a pressure of 200 kgf/cm<sup>2</sup>. Furthermore, the slip casted green body was fabricated with the dispersed yttria slurry. The slip casted body was dried at room temperature for 48 hours, and then dried in a dryer at 120 °C, for 24 hours. All three samples were sintered at 1650 °C, for 2 hours with a heating rate of 2 °C/min in an electric sintering furnace in an atmospheric condition.

### Characterization

The dispersion behavior of each slurry was investigated by measuring the height of the precipitate after standing for a certain time. The microstructure was examined using a SEM (Scanning Electron Microscope, JEOL/JSM-7100F) after Pt coating on the fracture surface of the green and sintered samples. The sintered density was measured by the Archimedes method, and the average value was used as data after measuring each specimen more than five times.

## Results and Discussion

The results of dispersion behavior according to the amount of dispersant are shown in Fig. 1. The slurry to which 0.2~0.6 wt% of dispersant was added began to precipitate within 5 minutes, and more than 16 ml (80%) precipitated after 12 hours. The slurry to which 0.8 wt% of dispersant was added precipitated about 3 ml (15%) initially, but after 12 hours, 9 ml had precipitated. The slurry to which 1.0 wt% or 1.2 wt%

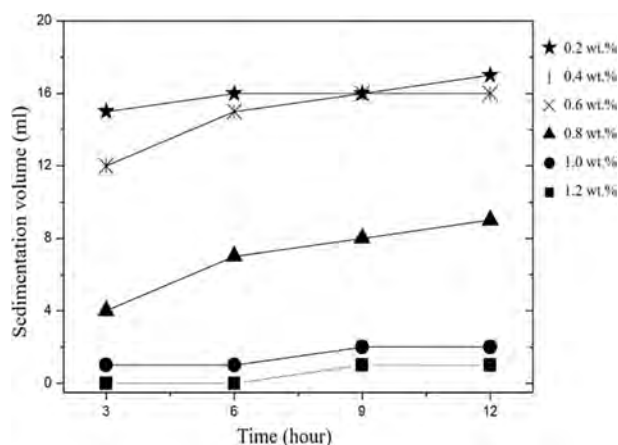
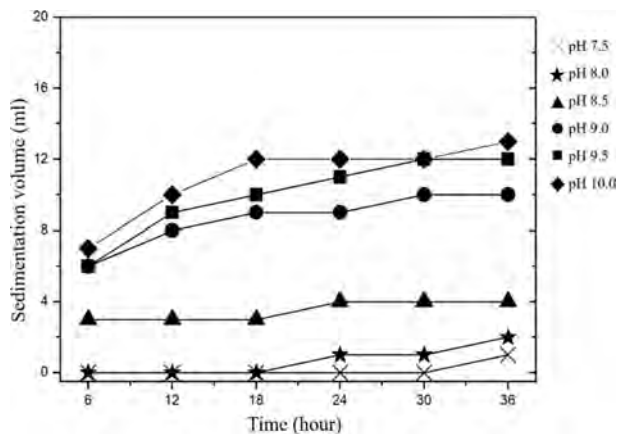


Fig. 1. Dispersion behavior of nano yttria slurry according to amount of dispersant.



**Fig. 2.** Dispersion behavior of nano yttria slurry according to pH condition.

of dispersant was added showed little precipitation after 6 hours. Finally, 2 ml precipitated in the case of the 1.0 wt% slurry and 1 ml precipitated for the 1.2 wt% slurry. As the amount of added dispersant was increased, the dispersion behavior was further improved. However, according to D. Huo [4], when the amount of dispersant increased, the particle growth during the sintering process might increase and thus the pore diffusion rate might not reach the movement speed of the grain boundary and the amount of pores is expected to increase. Therefore, in this experiment, the addition of 1.2 wt% dispersant was determined as the optimum condition.

The results of the dispersion behavior according to pH adjustment are shown in Fig. 2. The slurries of pH 9.0, 9.5 and 10.0 began to precipitate immediately from the beginning of the pH adjustment, and mostly yttria powders precipitated within 10 minutes. It was shown that gelation of the slurries of pH 7.5 and 8.0 readily occurred. For ordinary commercial yttria, the isoelectric point has a pH range of 8.5–9.0. However, the isoelectric point pH changes depending on the size of the particles and the type and amount of added dispersant. According to S. C. Santos et al. [16], when yttria powder having a particle size of 6.51  $\mu\text{m}$  and a specific surface area of 8.52  $\text{m}^2/\text{g}$  was dispersed in an aqueous system using the dispersant PAA, the isoelectric point pH was lowered as more dispersant was added. When no dispersant was added, the isoelectric point was at pH 8.5. In a study by J. He et al. [17], the zeta-potential was measured using yttria slurry containing powder having a particle size of about 33 nm and a specific surface area of 33.89  $\text{m}^2/\text{g}$  and TAC (Triammonium citrate) as the dispersant. Without TAC, the isoelectric point was at pH 6.0, and with TAC, the isoelectric point was at pH 5.8. As shown in these studies, with smaller particle size, the isoelectric point is located at accordingly lower pH. Since the particle size of the yttria powder used in this study is about 10–15 nm, it is estimated that the isoelectric point would be lower than pH 6.0. The

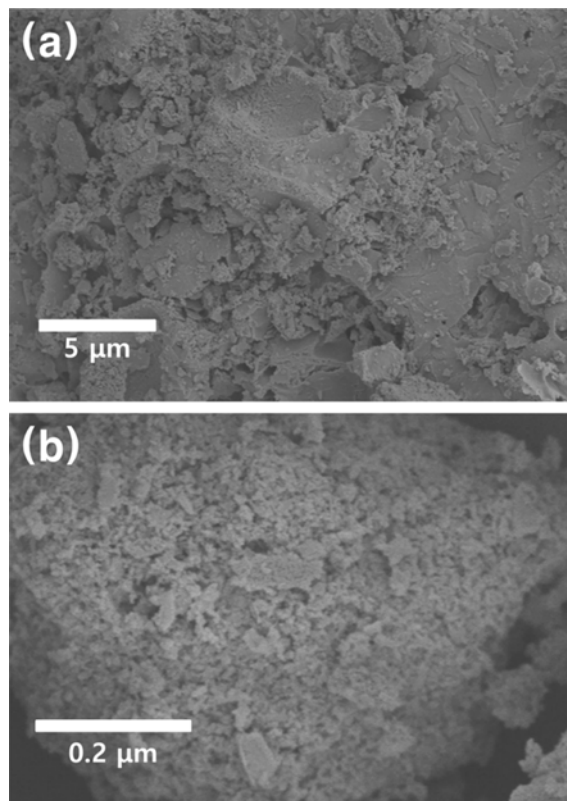


**Fig. 3.** SEM micrographs of fracture surface of uni-axially pressed nano yttria powder compact : (a)  $\times 3$  k, (b)  $\times 10$  k.

reason why gelation occurred is that ammonium acetate, a by-product of the neutralization reaction of ammonia and acetic acid, is produced with the addition of ammonia, and acetamide is produced by the heat of neutralization.

Gelation did not occur at pH 8.5 and no severe precipitation occurred, and thus it was selected as the best dispersion condition. Under this condition, no gelation would occur because the amount of added ammonia was small, and the heat of neutralization was small, and thus no acetamide was produced. Indeed, when a large amount of ammonia was added, steam was observed, but when a small amount was added, it was not observed. In order to lower the pH, the amount of ammonia added would be increased with increasing acetic acid solution, and thus the reaction byproducts of acetic acid and ammonia would also be increased.

The microstructures of the yttria green body fracture surfaces are shown in Figs. 3–5. Fig. 3 shows the fracture surface of the uniaxial pressed nano yttria powder compact. It shows severe agglomeration and a wide particle size distribution, and the powder packing is not constant. It is therefore estimated that large pores are irregularly distributed inside the compacts. In this case, it is expected that densification is difficult during sintering. It was confirmed that the nano-sized particles agglomerated in the form of large particles (Fig. 3 (b)). Fig. 4 shows the fracture surface of the gel powder compact. It was confirmed that most of the particles

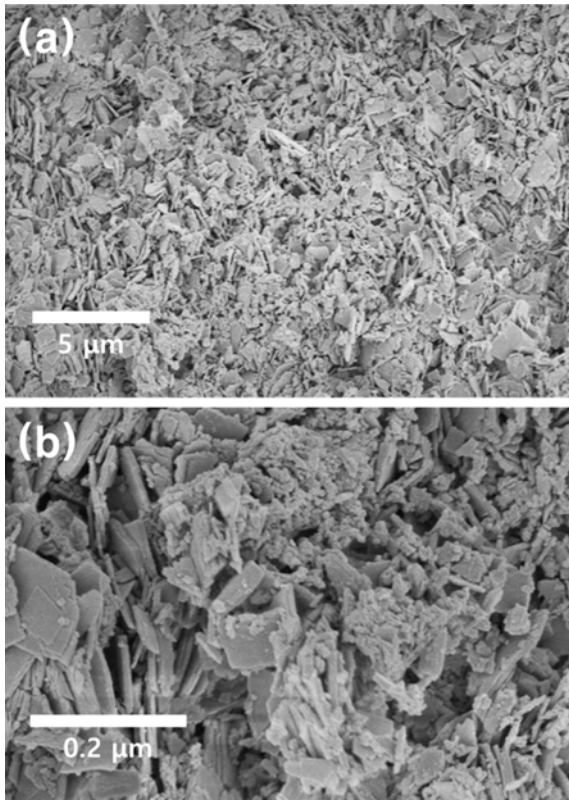


**Fig. 4.** SEM micrographs of fracture surface of uniaxially pressed, gel-type nano yttria powder compact : (a)  $\times 3$  k, (b)  $\times 10$  k.

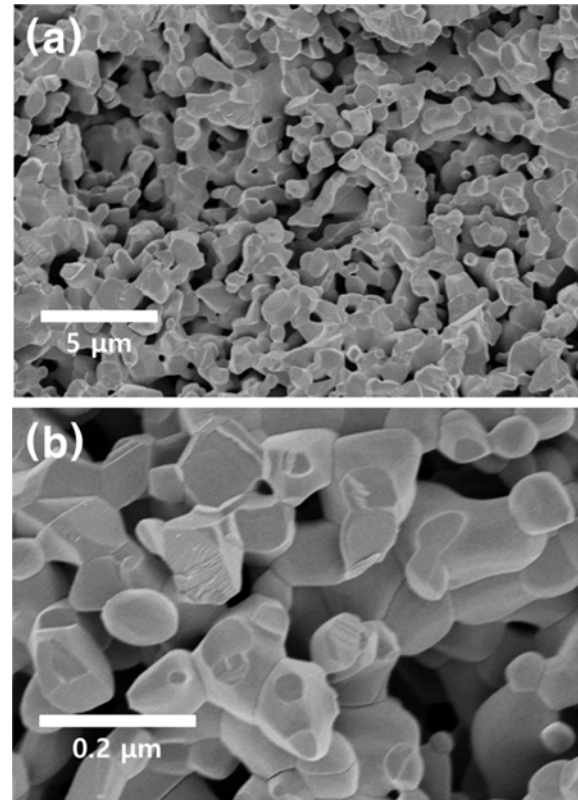


**Fig. 6.** SEM micrographs of fracture surface of sintered yttria prepared by uniaxial pressing with nano yttria powder : (a)  $\times 3$  k, (b)  $\times 10$  k.

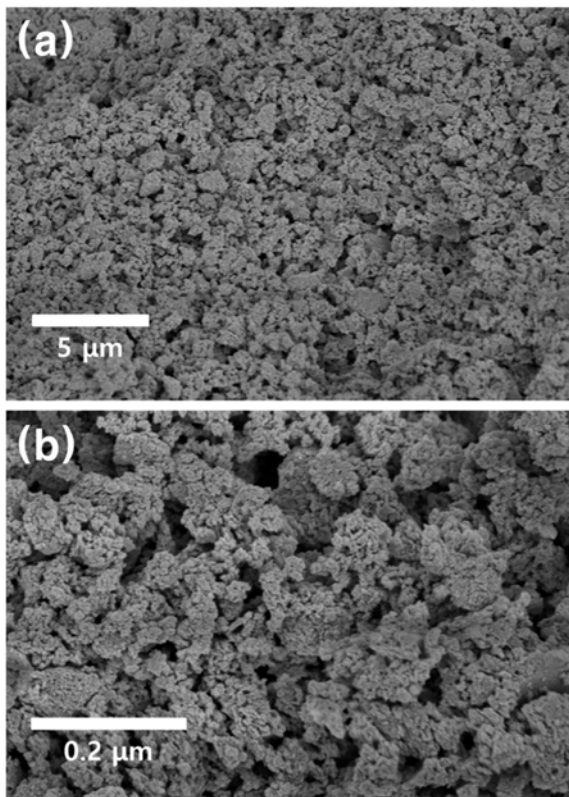


**Fig. 5.** SEM micrographs of fracture surface of nano yttria powder compact prepared by slip casting : (a)  $\times 3$  k, (b)  $\times 10$  k.

had a plate-like shape (Fig. 4 (b)), and the particle size distribution was relatively narrow. In the enlarged microstructure, plate-shaped particles and spherical nano-sized particles are present in the mixture. These fine particles were mainly present on the surface of the broken plate-shaped particles. It is estimated that the platelets were formed as the nano-sized yttria slurry gelled and dried. The powder having the plate-like shape did not exhibit severe agglomeration in comparison with the powder compact obtained from dry pressing with the nano-sized yttria particles. Irregular aggregation of the plate-shaped particles was hardly observed. The fracture surface microstructures of the slip casted green body are shown in Fig. 5. The fracture surface of the slip casted green body showed very homogeneous particle size compared with other samples, and was mostly spherical. Although a narrow range of aggregation was observed, a relatively homogeneous distribution was observed over a wide range.

The fracture surface microstructures of the sintered specimen according to different forming methods are shown in Figs. 6~8. As shown in Fig. 6, the sintered specimen derived from the dry pressing method had many pores, and partially sintered grains were observed. Most particles were about  $1.0\sim 2.0\ \mu\text{m}$  in size with peanut-shape particles. Compared with the fracture surface of the green body, notable grain growth was

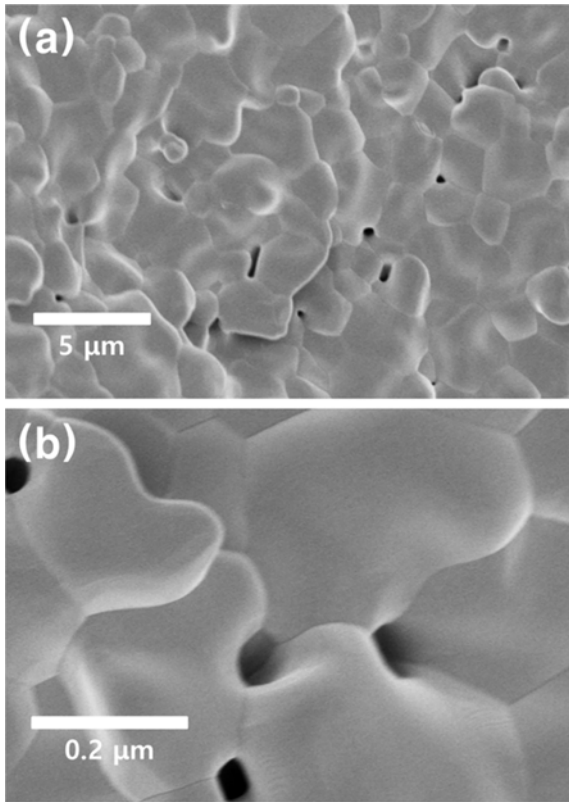


**Fig. 7.** SEM micrographs of fracture surface of sintered yttria prepared by uniaxial pressing with gel-type yttria powder : (a)  $\times 3$  k, (b)  $\times 10$  k.

occurred, but the microstructure was not very compact due to the wide distribution of pores. For the sintered specimen using the gel powder, there were almost no pores, and the grain growth was more developed (Fig. 7). The improved densification is ascribed to the elimination of agglomeration of the nano powder to some extent by applying the ball milling process to the prepared slurry, and agglomeration in the slurry was also prevented by applying the dispersant and pH control. The slip casting sintered specimen had almost no pores at the grain boundaries and spherical shape crystals were observed in the intragranular area (Fig. 8). In particular, the fracture surface showed intragranular fracture behavior and this means that grain boundary bonding occurred more strongly. It was estimated that this phenomenon derives from further progression of densification. The spherical shape crystals appear to be recrystallized yttria grains.

Table 1 shows the linear shrinkage and the relative density of each sintered body. The sintered body obtained from dry pressing the nano powder has a relative density of 82% with 26% shrinkage. The dry pressed nano powder compact (Fig. 3) has a wide range of particle size distribution from about large 5  $\mu\text{m}$  agglomerated particles to small 0.1  $\mu\text{m}$  particles. The macropores caused by the irregularities of agglomeration might affect the low density of the sintered body. The

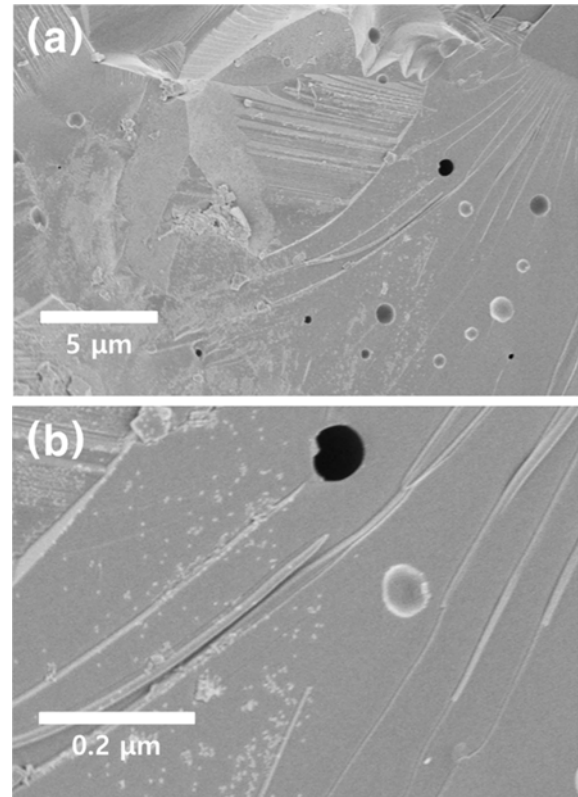


**Fig. 8.** SEM micrographs of fracture surface of sintered yttria prepared by slip casting with nano yttria powder : (a)  $\times 3$  k, (b)  $\times 10$  k.

**Table 1.** Shrinkage and relative density of sintered yttria according to various forming methods

	Linear shrinkage (%)	Relative Density (%)
Nano powder pressing	26	82
Gel powder pressing	38	93
Slip casting	41	98

sintered body obtained from the gel powder compact has a relative density of 93% with 38% shrinkage. Pores mainly existed at the grain boundary, which is estimated to be a result of the large pores in the powder compact not being removed during firing. The yttria sintered body prepared by slip casting has a relative density of 98% with 41% shrinkage. In the study of H. K. Lee et al. [18], it is surmised that for the growth of spherical grains, internal seeds are formed from a small amount of impurities as the grains grow, and then these seeds grow to form the spherical grains. All samples have very high sintering shrinkage in comparison with the sintering behavior of other ceramics. In the case of slip casting, the shrinkage was over 40%. This means that the voids between the homogeneous nano powder compact are relatively small and there are no large pores by agglomeration, and thus it is estimated that densification occurred as a result of substantial shrinkage.

## Conclusions

For the sintering of the 10 nm yttria powder, the sintering behavior was investigated using gel type powder compacts and slip casting compacts with aqueous slurries rather than conventional dry pressure compacts. By use of a dispersing agent and pH control, it was possible to prepare a properly dispersed nano yttria slurry. The green body prepared from the aqueous slurry had a sintering temperature of 1650 °C, and higher density than conventional dry pressure compacts. The problem of dry pressing with nano powder was solved by using the gel type powder. This gelation phenomenon was relatively easily obtained by pH control. In particular, the green body by slip casting had a relative density of 98% with 41% sintering shrinkage. Furthermore, unusual microstructure was observed where spherical-shape, recrystallized particles were observed on the intra-granular fracture surfaces.

## References

1. C.H. Jung, J.S. Jang, and S.J. Lee, *Met. Mater. Int.* 17[3] (2011) 451-455.
2. S.J. Lee and C.H. Jung, *J. Nanosci. Nanotechnol.* 12[1] (2012) 800-805.
3. J.H. Han, *J. Kor. Ceram. Soc.* 34[12] (1997) 1247-1253.
4. D. Huo, Y. Zheng, X. Sun, X. Li, and S. Liu, *J. Rare. Earth*, 30[1] (2012) 57-62.
5. Y. Xu, X. Mao, J. Fan, X. Li, M. Feng, B. Jiang, F. Lei, and L. Zhang, *Ceram. Int.* 43[12] (2017) 8839-8844.
6. B.Y. Son and M.E. Jung, *Kor. J. Mater. Res.* 21[8] (2011) 444-449.
7. F.M.B. Marques and G.P. Wirtz, *J. Am. Ceram. Soc.* 74[3] (1991) 598-605.
8. C. Brecher, G.C. Wei, and W.H. Rhodes, *J. Am. Ceram. Soc.* 73[6] (1990) 1473-1488.
9. R.V. Mangalaraja, J. Mouzon, P. Hedstrom, S. Ananthakumar, and M. Odén, *Powder Technol.* 191[3] (2009) 390-314.
10. A.L. Micheli, D.F. Dungan, and J.V. Mantese, *J. Am. Ceram. Soc.* 75[3] (1992) 709-711.
11. Y. Huang, D. Jiang, J. Zhang, Q. Lin, and Z. Huang, *J. Am. Ceram. Soc.* 93[10] (2010) 2964-2967.
12. C.W. Park, J.H. Park, H.S. Kang, H.A. Lee, J.H. Lee, J.H. In, and K.B. Shim, *J. Ceram. Process. Res.* 19[5] (2018) 383-387.
13. L. Gan, Y.J. Park, H. Kim, J.M. Kim, J.W. KO, and J.W. Lee, *Int. J. Appl. Ceram. Tec.* 13[4] (2016) 678-684.
14. S.J. Lee, P. Thiyagarajan, and M.J. Lee, *J. Ceram. Process. Res.* 9[4] (2008) 385-388.
15. Y.K. Yang and S.J. Lee, *Arch. Metall. Mater.* 63[3] (2018) 1473-1476.
16. S.C. Santos, L.F. G. Setz, C. Yamagata, and S.R.H. de Mellocastanho, *Mater. Sci. Forum*, 660-661 (2010) 712-717.
17. J. He, X. D. Li, J. G. Li, and X. D. Sun, *Int. J. Mater. Sci. Eng.* 1[1] (2013) 28-31.
18. H.K. Lee, S.S. Lee, B.R. Kim, T.E. Park, and Y.H. Yun, *J. Korean. Cryst. Growth and Cryst. Technol.* 24[6] (2014) 268-273.